Journal of Luminescence 168 (2015) 236–240

Contents lists available at ScienceDirect

Journal of Luminescence

journal homepage: www.elsevier.com/locate/jlumin

Analysis of glow curve of $GaS_{0.5}Se_{0.5}$ single crystals

Mehmet Isik [a,*], Serdar Delice [b], Nizami Gasanly [b,c]

[a] Department of Electrical and Electronics Engineering, Atilim University, 06836 Ankara, Turkey
[b] Department of Physics, Middle East Technical University, 06800 Ankara, Turkey
[c] Virtual International Scientific Research Centre, Baku State University, 1148 Baku, Azerbaijan

ARTICLE INFO

Article history:
Received 21 April 2015
Received in revised form
23 June 2015
Accepted 28 July 2015
Available online 11 August 2015

Keywords:
Semiconductors
Chalcogenides
Defects
Thermoluminescence

ABSTRACT

Characterization of shallow trapping centers in $GaS_{0.5}Se_{0.5}$ crystals grown by a Bridgman method was carried out in the present work using thermoluminescence (TL) measurements performed in the low temperature range of 10–300 K. The activation energies of the trapping centers were obtained under the light of results of various analysis methods. The presence of three trapping centers located at 6, 30 and 72 meV was revealed. The analysis of the experimental glow curve gave reasonable results under the model that assumes slow retrapping which states the order of kinetics as $b=1$. Heating rate dependence of the observed TL peaks was studied for the rates between 0.4 and 1.0 K/s. Distribution of the traps was also investigated using an experimental technique based on the thermal cleaning of centers giving emission at lower temperatures. The distributed levels with activation energies increasing from 6 to 136 meV were revealed by increasing the stopping temperature from 10 to 52 K.

1. Introduction

A(III) B(VI)-type semiconducting compounds, GaX (X=S, Se), have been promising candidates to be used in optoelectronic devices in red and blue visible region [1–3]. In the crystal structure of these layered type semiconductors, lattices have strong ionic-covalent intralayer and weak van der Waals interlayer interactions [4]. Optical and electrical properties of these compounds have been investigated to have a foresight about the potential usefulness in relevant technological areas. The band gap energy of GaSe has been reported as ~2.0 eV [5,6]. The studies on the far-infrared conversion applications of GaSe showed that crystals transmitted light between 650 to 18,000 nm range which is wider and more appropriate than the range of other nonlinear optical materials, such as $AgGaSe_2$, $ZnGeP_2$, Tl_3AsSe_3 crystals [7]. GaS is a wide band gap semiconducting material having indirect and direct band gap energies of ~2.59 and 3.04 eV, respectively, at room temperature [8]. Therefore, it is a promising material for near-blue light emitting devices. Moreover, GaS crystals exhibit electroluminescence and photoluminescence in the green-blue region [2,9–10].

GaS_xSe_{1-x} mixed crystals are formed from GaSe and GaS without restrictions on the concentration of the constituent compounds ($0 \le x \le 1$) [11–13]. Taking into consideration the technological applications of GaSe and GaS, GaS_xSe_{1-x} mixed crystals can be important candidate to be used in the fabrication of long-pass filter, light emitting devices and optical detecting systems. Optical properties of GaS_xSe_{1-x} mixed crystals ($0 \le x \le 0.5$) grown by a Bridgman method were studied by transmission and piezoreflectance measurements [11]. The analysis of the obtained spectra showed that band gap energy increases from 1.986 eV (GaSe) to 2.37 eV ($GaS_{0.5}Se_{0.5}$). Photoluminescence measurements showed full-range luminescence of 625–480 nm from mixed crystals for $0 \le x \le 1$ at room temperature [14]. The Raman spectra of the mixed crystals for a wide range of composition ($0 \le x \le 1$) were obtained at 300 and 10 K [15].

Among GaS_xSe_{1-x} mixed crystals in the limits of solubility ($0 \le x \le 1$), $GaS_{0.5}Se_{0.5}$ crystal ($x=0.5$) is the most distinctive one showing properties of GaSe and GaS. The $GaS_{0.5}Se_{0.5}$ crystals, like binary compounds GaSe and GaS, have a layered structure [16,17]. Each layer has four atomic planes with the sequence Se(S)–Ga–Ga–Se(S). In general, constituent compounds, GaSe and GaS, are crystallized in the ε, γ and β-modifications, respectively. However, X-ray diffraction patterns showed that the intermediate compound $GaS_{0.5}Se_{0.5}$ contains two different layer types of ε- and β-modifications [18]. The primitive unit cell consists of four formula units from two neighboring layers (Fig. 1). The optoelectronic properties of semiconductors are affected due to the defects and impurities. Thermoluminescence (TL), thermally stimulated current (TSC) and photoluminescence (PL) are basic experimental techniques used for long times to characterize energy levels created due to the presence of defects and/or impurities. Previously,

* Corresponding author. Tel.: +90 312 5868552; fax: +90 312 5868091.
E-mail address: mehmet.isik@atilim.edu.tr (M. Isik).

http://dx.doi.org/10.1016/j.jlumin.2015.07.042
0022-2313/

we have reported the results of PL and TSC experiments. It was revealed that two observed bands in PL spectra are arising due to the radiative transitions from shallow donor levels located at 0.029 and 0.040 eV to deep acceptor levels located at 0.185 and 0.356 eV [19]. The activation energies of three trapping centers in $GaS_{0.5}Se_{0.5}$ were found as 0.072, 0.100 and 0.150 eV from the analysis of TSC measurements [20]. We expand our studies on the defect/impurity characterization of $GaS_{0.5}Se_{0.5}$ single crystals by carrying out TL experiments in the 10–300 K temperature range. Applying TL technique and investigating the differences with the results of PL and TSC analysis will provide a worthwhile data for a better understanding of defects and/or impurities in $GaS_{0.5}Se_{0.5}$ crystals.

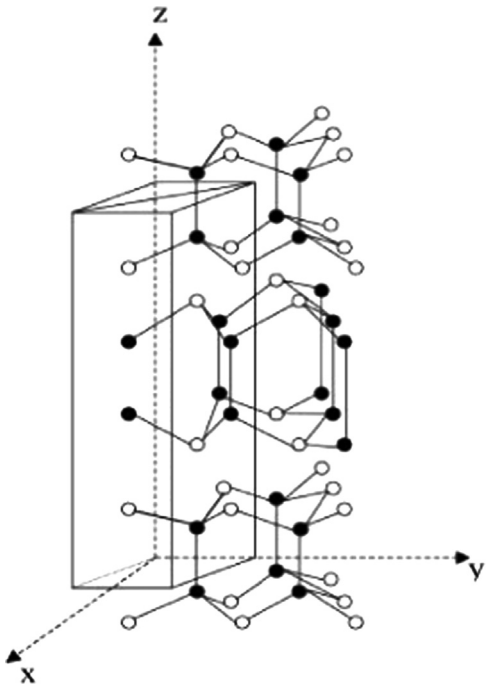

Fig. 1. The unit cell of $GaS_{0.5}Se_{0.5}$ crystal. Closed and open circles represent Ga and Se(S) atoms, respectively.

2. Experimental details

$GaS_{0.5}Se_{0.5}$ polycrystals were synthesized from high-purity elements (at least 99.999%) prepared in stoichiometric proportions. Single crystals of $GaS_{0.5}Se_{0.5}$ were grown by the Bridgman method in evacuated (10^{-5} Torr) silica tubes (10 mm in diameter and about 25 cm in length) with a tip at the bottom in our crystal growth laboratory. The ampoule was moved in a vertical furnace through a thermal gradient of 30 °C/cm, between the temperatures 1000 and 650 °C at a rate of 0.5 mm/h. The resulting ingots (orange in color) showed good optical quality and were easily cleaved along the planes that are perpendicular to the *c*-axis of the crystal. The chemical composition of the crystals was determined using the energy dispersive spectroscopy (EDS) experiments which were performed by a JSM-6400 scanning electron microscope having two equipments called as "Noran System6 X-ray microanalysis system" and "Semafore Digitizer" which take part in the analysis of experimental data.

Thermoluminescence measurements were carried out using home made experimental set-up (see Fig. 2) which was built around a closed cycle helium gas cryostat (Advanced Research Systems, Model CSW-202). A Lakeshore Model 331 temperature controller was used to adjust the sample temperature in the 10–300 K range. A photomultiplier tube, a blue light source (~470 nm) and the relevant optics were connected to the optical access port of the cryostat (quartz window) by a measurement chamber. Luminescence emitted from the crystal was focused by lenses on the photomultiplier tube (Hamamatsu R928; spectral response: 185–900 nm) working in photon counting regime. Pulses from the photomultiplier tube were converted into TTL pulses using a fast amplifier/discriminator (Hamamatsu Photon Counting Unit C3866) and counted by the counter of the data acquisition module (National Instruments, NI-USB 6211). A software program written in LabView™ graphical development environment was used to control whole measurement system/devices. The sample was illuminated at 10 K for 600 s, experimentally determined time

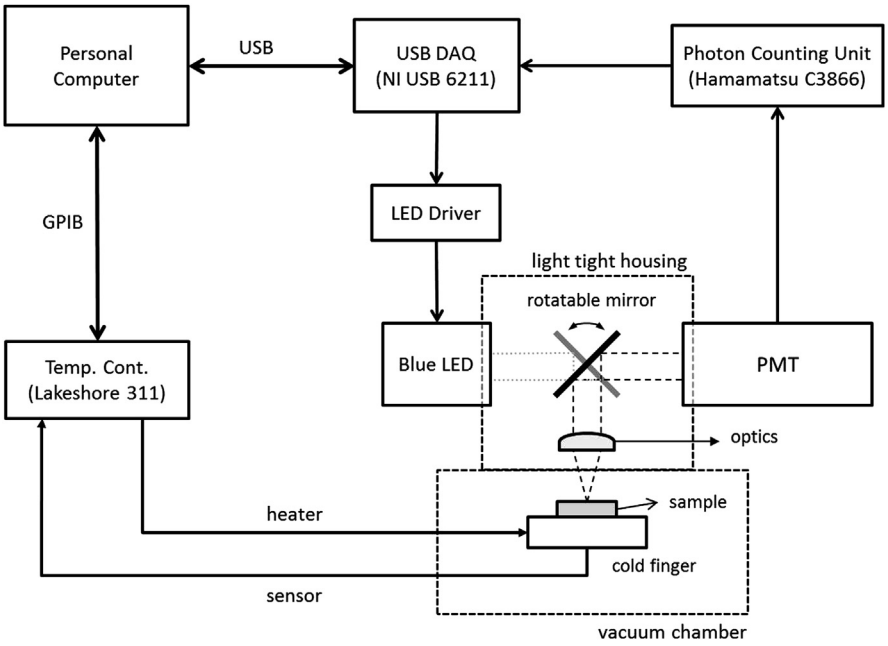

Fig. 2. Simplified block diagram of the TL measurement set-up.

to fill the traps completely. Then, after 120 s of waiting, the sample was heated at a constant heating rate and the emitted photon counts were recorded as a function of temperature.

3. Results and discussion

Fig. 3 shows the EDS results used to determine the chemical composition of the crystal. Since every element has distinctly unique energy levels, each element produces characteristic X-rays which get an opportunity to determine the elemental composition of the sample by analyzing the spectra [21]. The atomic composition ratio of constituent elements in the mixed crystal was determined from the relative counts of the detected X-rays. The emission energies for Ga, S and Se elements are equal to (1.098, 1.125, 1.144, 1.171 and 9.241 keV), (0.163, 0.164, 2.307, 2.464 and 2.470 keV) and (1.379, 1.419, 1.434 and 1.475 keV), respectively [22]. EDS measurements showed that the atomic composition ratio of the studied sample Ga:S:Se was found to be 49.8:24.8:25.4, respectively.

Fig. 4 shows the TL spectra of $GaS_{0.5}Se_{0.5}$ crystal obtained at β=0.4 K/s heating rate. Although the experiments were carried out in the 10–300 K temperature range, this figure represents the spectra for the range in which TL peaks were observed. The analysis of the obtained experimental data was accomplished using a curve fitting method [23]. In this method, TL glow curve is fitted using a software program under the light of theoretical expression

$$I_{TL} = n_0 s \exp\left\{ -\frac{E_t}{kT} - \int_{T_0}^{T} \frac{s}{\beta} \exp(-E_t/kT)dT \right\} \quad \text{(for first-order kinetics)} \tag{1}$$

$$I_{TL} = n_0 s \exp\left(-\frac{E_t}{kT} \right) \left[1 + (b-1)\frac{s}{\beta} \int_{T_0}^{T} \exp(-E_t/kT)dT \right]^{-\frac{b}{b-1}} \quad \text{(for non first-order kinetics)} \tag{2}$$

which gives the TL intensity (I_{TL}) as a function of temperature (T) for the negligible and non-negligible retrappings, respectively [24]. E_t, s, n_0 and b are the activation energy, attempt-to-escape frequency, initial concentration of the charge carriers in the trap level(s) and order of kinetics, respectively. The fitting process was successfully resulted with the presence of three trapping centers located at 6 ± 0.5, 30 ± 2 and 72 ± 4 meV under the light of Eq. (1) (solid line in Fig. 4). The good agreement between the experimental glow curve and fitted curve obtained using Eq. (1) confirms that the order of kinetics is equal to 1 corresponding to slow retrapping process. The reliability of the curve fitting method is thought as decreasing with increasing fitting parameters which is proportional to the number of peaks. Therefore, we have also performed the analysis on the glow curve in which shallowest trapping center was emptied using a thermal cleaning method [23]. The fitting (dash-dot line) of the thermally cleaned TL glow curve (triangles in Fig. 4) was resulted for remaining peaks with 30 and 74 meV activation energies which can be thought as a powerful indication of accuracy of results. At this point, it will be worthwhile to compare these energies with previously reported energy values obtained from the analysis of PL and TSC measurements [19,20]. Taking into account the possible errors, the energy values of 30 and 29 meV obtained from TL and PL analyzes, respectively, can be assigned to the same level. This level is partially compensated allowing for both PL and TL emissions. Moreover, trapping center with 72 meV activation energy is taking role in both of TL and TSC processes. Other two centers revealed in TSC experiments located at 100 and 150 meV were not observed in TL spectra. We suppose that trapped carriers in these levels recombine with opposite carrier in the recombination center by making non-radiative transition.

The results of the curve fitting method can also be used to calculate the attempt-to-escape frequency (s) and capture cross section (S_t) of the revealed traps [25]. The values of s and S_t are given in Table 1. From this table, it can be noticed that the values of the frequency factors are by far lower than usually expected value of $\sim 10^{12}$ s^{-1} [24]. In the literature, the low-frequency factors have been previously reported in papers on ZnO/Au/ZnS/Au (0.15 and 5.55 s^{-1}) [26], $Zn_{1-x}Cd_xO$ (1.67 and 12.52 s^{-1}) [27],

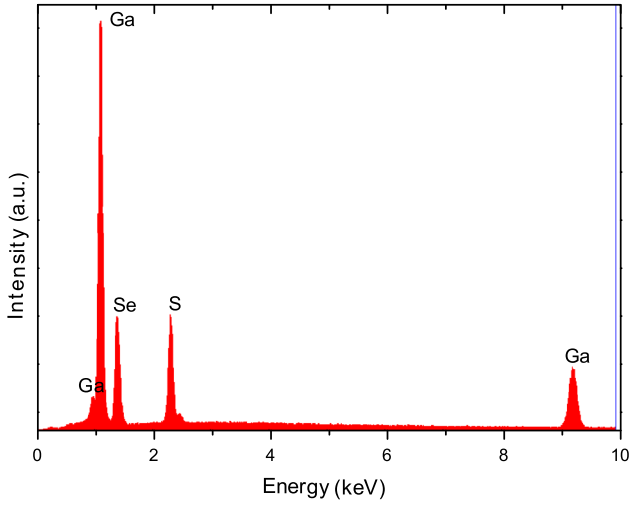

Fig. 3. Energy dispersive spectroscopic analysis of $GaS_{0.5}Se_{0.5}$ crystal.

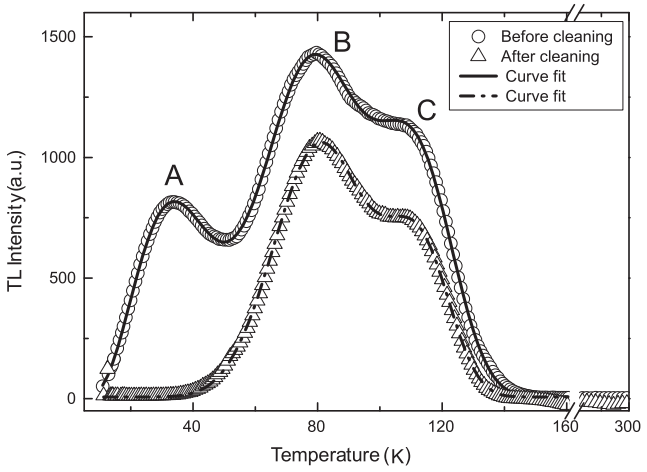

Fig. 4. Experimental TL glow curves of $GaS_{0.5}Se_{0.5}$ crystal with heating rate of 0.4 K/s before (circles) and after (triangles) thermal cleaning. Solid and dash dot curves show the fits to the experimental data.

Table 1
Activation energy (E_t), capture cross section (S_t) and attempt-to-escape frequency (s) of revealed traps in $GaS_{0.5}Se_{0.5}$ crystals.

T_m (K)	E_t (meV)			S_t (cm^2)	s (s^{-1})
	Curve fit method		Heating rate method		
	Before cleaning	After cleaning			
33.5	6 ± 0.5	–	7	1.3×10^{-25}	1.2
79	30 ± 2	30 ± 2	32	2.2×10^{-25}	2.8
108	72 ± 4	74 ± 4	–	4.2×10^{-24}	65.6

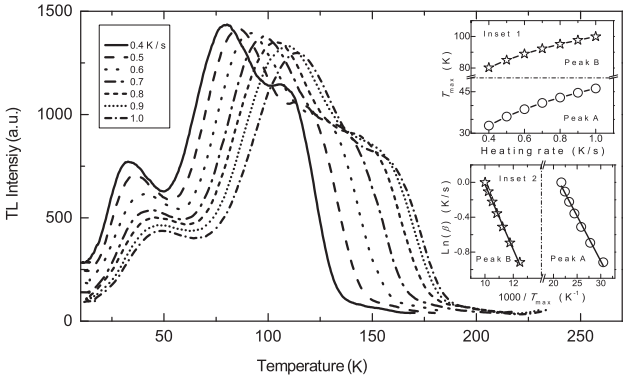

Fig. 5. Experimental TL curves of $GaS_{0.5}Se_{0.5}$ crystal with different heating rates. Inset 1: Dependence of peak maximum temperatures on heating rate. Inset 2: The plot of $\ln(\beta)$ vs. $1000/T_m$. Circles/stars and solid lines represent the experimental data and their linear fits, respectively.

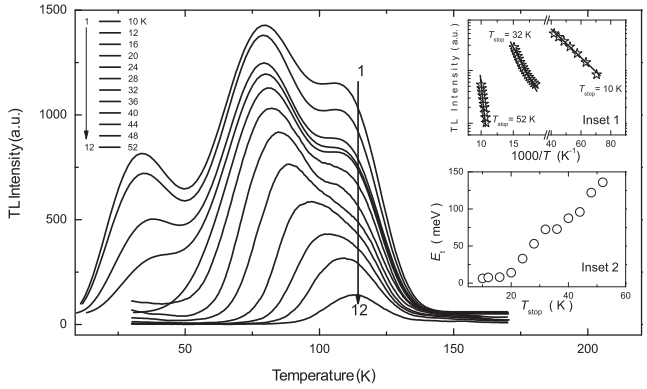

Fig. 6. The glow curves of $GaS_{0.5}Se_{0.5}$ crystals at different T_{stop} temperatures at heating rate $\beta=0.4$ K/s. Inset 1: TL intensity vs. $1000/T$. The stars present the experimental data and the lines represent the theoretical fits using the initial rise method. Inset 2: The dependence of activation energies on T_{stop} values.

$TlInS_2$ (1.5 and 10.1 s^{-1}) [28] and 10 s^{-1} (Polystyrene) [29]. The extremely low values of attempt-to-escape frequencies can be attributed to the strong repulsive barrier to capture the carriers which is characteristic feature of the system with disorder-like structure [30,31].

The heating rate dependence of the TL glow curve was investigated for rates between 0.4 and 1.0 K/s (see Fig. 5). Peak maximum temperatures (T_m) of the peaks shifted to higher temperatures in accordance with theoretical approach given by Chen and McKeever (inset 1 of Fig. 5) [24]. Thermal activation energy of a trapping center can also be calculated taking advantage of heating rate dependence of TL glow curves. In the thermally stimulated phenomena, the dependence of heating rate on T_m is given as [25]

$$\beta = (sk/E_t)T_m^2 \exp(-E_t/kT_m). \quad (3)$$

In the right hand side of Eq. (3), exponential term is the dominant T_m dependent factor rather than the T_m^2 term. Therefore, the plot of $\ln(\beta)$ vs. $1/T_m$ gives a line with a slope of $-E_t/k$. Inset 2 of Fig. 5 shows these plots (circles/stars) and their linear fits (solid lines) for peaks A and B. Since the T_m value of the peak C is not clearly determined from the glow curve, we have left this peak out of heating rate dependence analysis. The activation energy values were obtained from the slope as $E_{tA}=7$ meV and $E_{tB}=32$ meV. These results are in good agreement with those obtained from curve fitting method.

The foregoing results are related to the case of presence of discontinuous localized states having single valued energy. However, traps associated with certain defects and/or impurities can have wide range of distribution in highly defective structured crystals. In order to investigate distribution of trapping centers, an experimental technique based on thermally cleaning of the centers giving emission at lower temperatures and obtaining TL glow curve associated with remaining centers was applied [25,32]. This technique ($T_m(E_t)$–T_{stop}) was applied as follows: the sample was illuminated at low temperature ($T_0=10$ K) and heated at a constant heating rate ($\beta=0.4$ K/s) up to a temperature (T_{stop}). Then the sample was cooled to T_0 temperature and TL experiments were performed in the whole temperature range (10–300 K) without additional illumination. Since the trapping centers giving emission below T_{stop} temperature were fully or partially emptied, the new TL curve carries the characteristics of remaining deeper trapping centers. Fig. 6 shows TL curves obtained after applying the mentioned technique for different T_{stop} values between 10 and 52 K. The activation energy of the shallowest level in each TL glow curve was calculated using an initial rise method. In this method, the initial part of the TL peak (up to ~10% of its peak maximum intensity) is proportional to $\exp(-E_t/kT)$ when the trapped carriers are excited to the non-localized states [25]. When the initial portion of the curve was analyzed, $\ln(I_{TL})$ vs. $1/T$ graph gives a straight line with a slope of $(-E_t/k)$. Although, a traps distribution case is considered in the above mentioned process, the initial rise method gives one activation energy value. Hornyak and Chen reported the obtained energy from the initial rise method as centered energy value of continuous distribution of activation energies in an energy range [33]. Therefore, the previously obtained energies from curve fitting method are attributed to the centered energy value (or mean energy of distribution) of three discrete trapping centers. Inset 1 of Fig. 6 represents the corresponding plots of the experimental data (stars) and their linear fits (solid lines) for three measurements. Inset 2 of Fig. 6 shows the T_{stop} dependence of activation energies. The increase of activation energy from 6 to 14 meV can be associated to the traps distribution of shallowest level (peak A). The remaining increasing energies from 33 to 136 meV are related to the distribution of peaks B and C. Since these peaks are closely overlapped, we assume that excitation of trapped charge carriers can occur from both of the centers for some T_{stop} values. Therefore, we avoid giving specific energy ranges of distribution of traps for these centers.

4. Conclusion

Thermoluminescence experiments performed on $GaS_{0.5}Se_{0.5}$ single crystals exhibited one broad glow curve consisting three individual peaks at 33, 79 and 108 K. Activation energy values of trapping centers associated with these peaks were found from the curve fitting method as 6, 30 and 72 meV. Analysis showed that slow retrapping (first order of kinetics) is the dominant mechanism in TL processes. The behavior of the TL glow curves in relation to different heating rate showed that as heating rate increases peak maximum temperature shifts to higher values and intensity of glow curve decreases. Activation energies of shallowest two centers were found as 7 and 32 meV from heating rate dependency of peak maximum temperature. Distribution of the traps was also investigated using $T_m(E_t)$–T_{stop} technique. The distributed levels with activation energies increasing from 6 to 136 meV were revealed by increasing the stopping temperature from 10 to 52 K.

References

[1] G. Micocci, A. Serra, A. Tepore, J. Appl. Phys. 82 (1997) 2365.
[2] A. Cingolani, A. Minafra, P. Tantalo, C. Paorici, Phys. Status Solidi A 4 (1971) K83.

[3] M. Somogyi, Phys. Status Solidi A 7 (1971) 263.
[4] M. Balkanski, R.F. Wallis, Semiconductor Physics and Applications, Oxford University Press, Oxford, 2000.
[5] S. Shigetomi, T. Ikari, H. Nakashima, J. Appl. Phys. 74 (1993) 4125.
[6] A.G. Kyazym-zade, R.N. Mekhtieve, A.A. Akhmedov, Sov. Phys. Semicond. 25 (1991) 840.
[7] N.B. Singh, D.R. Suhre, V. Balakrishna, M. Marable, R. Meyer, N. Fernelius, F.K. Hopkins, D. Zelmon, Prog. Cryst. Growth Charact. Mater. 37 (1998) 47.
[8] E. Auclich, J.L. Brebner, E. Mooser, Phys. Status Solidi B 31 (1969) 129.
[9] G. Akhundov, I.G. Aksyanov, G.M. Gasumov, Sov. Phys. Semicond. 3 (1969) 767.
[10] M.I. Karaman, V.P. Mushinskii, Sov. Phys. Semicond. 4 (1970) 662.
[11] C.C. Wu, C.H. Ho, W.T. Shen, Z.H. Cheng, Y.S. Huang, K.K. Tiong, Mater. Chem. Phys. 88 (2004) 313.
[12] A. Masui, S. Onari, K.R. Allakhverdiev, F. Gashimzade, T. Mamedov, Phys. Status Solidi B 223 (2001) 139.
[13] M.A. Osman, Physica B 275 (2000) 351.
[14] C.H. Ho, K.W. Huang, Solid State Commun. 136 (2005) 591.
[15] N.M. Gasanly, J. Raman Spectrosc. 36 (2005) 879.
[16] A. Kuhn, A. Chevy, R. Chevalier, Phys. Status Solidi A 36 (1976) 181.
[17] A. Kyazim-zade, N.M. Mekhtiev, Z.S. Samedov, V.I. Tagirov, Sov. Phys. Solid State 26 (1983) 737.
[18] C.H. Ho, C.C. Wu, Z.H. Cheng, J. Cryst. Growth 279 (2005) 321.
[19] A. Aydinli, N.M. Gasanly, K. Goksen, Mater. Res. Bull. 36 (2001) 1823.
[20] A. Aydinli, N.M. Gasanly, S. Aytekin, Solid State Commun. 132 (2004) 857.
[21] J.J. Friel, X-Ray and Image Analysis in Electron Microscopy, Princeton Gamma-Tech, Princeton, 2003.
[22] J. Goldstein, D. Newbury, D. Joy, C. Lyman, P. Echlin, E. Lifshin, L. Sawyer, J. Michael, Scanning Electron Microscopy and X-Ray Microanalysis, Springer Science, LLC, New York, 2007.
[23] N.S. Yuksek, N.M. Gasanly, H. Ozkan, Semicond. Sci. Technol. 18 (2003) 834.
[24] R. Chen, Y. Kirsh, Analysis of Thermally Stimulated Processes, Pergamon Press, Oxford, 1981.
[25] R. Chen, S.W.S. McKeever, Theory of Thermoluminescence and Related Phenomena, World Scientific, Singapore, 1997.
[26] E. Turan, M. Zor, A.S. Aybek, M. Kul, Physica B 395 (2007) 57.
[27] A.S. Aybek, N. Baysal, M. Zor, E. Turan, M. Kul, J. Alloy. Compd. 509 (2011) 2530.
[28] S. Ozdemir, R.A. Suleymanov, E. Civan, T. Firat, Solid State Commun. 98 (1996) 385.
[29] L.F. Pender, R.J. Fleming, J. Phys. C: Solid State Phys. 10 (1977) 1571.
[30] T. Datta, R. Noufi, S.K. Deb, J. Appl. Phys. 59 (1986) 1548.
[31] D.C. Look, Z.Q. Fang, W. Kim, O. Aktas, A. Botchkarev, A. Salvador, H. Morkoc, Appl. Phys. Lett. 68 (1996) 3775.
[32] S.R. Anishia, M.T. Jose, O. Annalakshmi, V. Ramasamy, J. Lumin. 131 (2011) 2492.
[33] W.F. Hornyak, R. Chen, J. Lumin. 44 (1989) 73.